Quantum Electronics **48** (8) 695–698 (2018)

https://doi.org/10.1070/QEL16716

Spectroscopic and laser characteristics of ceramics based on Yb^{3+}-doped $Lu_2O_3-Y_2O_3$ solid solution

R.N. Maksimov, V.A. Shitov, M.R. Volkov, O.L. Vadimova, I.L. Snetkov

Abstract. **We report on quasi-cw lasing at a wavelength of 1031 nm with a maximum power of 8 W and a slope efficiency of 32.3% achieved in a thin-disk ceramic element based on ytterbium-doped solid solution of yttrium and lutetium sesquioxides. A sample of Yb : (Lu, Y)$_2$O$_3$ ceramics was fabricated by solid-state sintering of nanosized particles of a predetermined composition synthesised by laser ablation. The study of the spectral and luminescent characteristics of the obtained ceramics shows that partial substitution of Y^{3+} cations by Lu^{3+} cations broadens the absorption, luminescence, and laser spectra and shifts their peaks with respect to those of $Yb:Y_2O_3$ ceramics.**

Keywords: *nanopowder, optical ceramic, solid solution, ytterbium, emission spectrum, laser oscillation.*

1. Introduction

In the recent decade, much attention has been paid to the development of near-IR solid-state lasers with a high peak power. This is first of all caused by a wide application of these laser systems in industry for remote cutting, welding, hardening, thermal treatment, and marking of various materials [1–3], as well as in fundamental scientific studies on initiation and maintenance of thermonuclear fusion [4–6]. One of the key components of solid-state lasers with a high peak power is an active medium in which a population inversion of laser levels is formed. This medium should have a broad gain band, because the pulse duration is inversely proportional to the spectral width of the laser line.

It should be noted that Yb^{3+}-doped ceramics are today preferable materials for lasers with high average and peak powers simultaneously. This is explained, first, by the three-level energy diagram and a low quantum defect of the Yb^{3+} ion, which leads to a relatively low heat release in the process of lasing, as well as by its rather high absorption and gain cross sections and broad spectrum sufficient for generation of picosecond pulses. Second, optical ceramics have such advantages over single crystals of similar composition as large sizes, better thermomechanical characteristics, simple production, lower energy consumption and cost, possibility of forming multilayer and multicomponent structures, and a gradient distribution of active centres [7–11].

Using ceramics based on ytterbium-doped yttrium oxide ($Yb:Y_2O_3$), which has a rather broad gain band, the authors of [12] achieved record-short (68-fs) pulses with an average power of 540 mW at a wavelength of 1036 nm. In the same work, 53-fs pulses with an average power of 1 W at a wavelength of 1042 nm were obtained in a combined ceramic medium consisting of two successive layers, $Yb:Sc_2O_3$ and $Yb:Y_2O_3$, connected with each other via an optical contact, with a total gain band width of 27.3 nm. Such a broad emission band is obtained due to a local overlap of two emission spectra of Yb^{3+} ions in different crystal matrices (Y_2O_3 and Sc_2O_3).

In addition to successive layers of laser media, a promising way to decrease the pulse duration is creation of materials based on solid solutions of two and more oxides. Applicability of this method was previously demonstrated by us in [13] and by other authors investigating the spectroscopic and laser characteristics of single- and polycrystalline materials based on mixed oxides $Lu_2O_3-Sc_2O_3$ and $Lu_2O_3-Sc_2O_3-Y_2O_3$ doped with Yb^{3+} or Tm^{3+} ions [14, 15]. However, the current literature provides scarce information about the spectral characteristics of $Lu_2O_3-Y_2O_3$ solid solutions.

In the present work, we comparatively analyse the spectroscopic properties and lasing characteristics of $Yb:(Lu,Y)_2O_3$ ceramics and a one-component $Yb:Y_2O_3$ sample.

2. Synthesis of ceramic samples and study of their spectral and luminescent characteristics

The studied ceramic samples were synthesised at the Institute of Electrophysics, Ural Branch, Russian Academy of Sciences, by solid-phase sintering of nanopowders of a complex chemical composition. Nanoparticles synthesised by laser ablation [16, 17] were used as initial materials. The solid targets were made of microsized Yb_2O_3, Y_2O_3, and Lu_2O_3 powders with the base material concentration no lower than 99.95%, which were mixed to obtain $Yb_{0.06}Y_{1.94}O_3$ and $Yb_{0.1}Lu_{0.3}Y_{1.6}O_3$ powders with addition of ZrO_2 (5 mol %) as a sintering additive. Analysis with the use of an Optima 2100 DV mass-spectrometer showed that, in the process of laser synthesis, the nanopowders are enriched with the most fusible component (Yb_2O_3), and the final ceramics compositions are $Yb_{0.075}Y_{1.843}Zr_{0.082}O_{3-\delta}$ and $Yb_{0.118}Lu_{0.238}Y_{1.565}Zr_{0.079}O_{3-\delta}$.

R.N. Maksimov Institute of Electrophysics, Ural Branch, Russian Academy of Sciences, ul. Amundsena 106, 620016 Ekaterinburg, Russia; Ural Federal University named after the First President of Russia B.N. Yeltsin, ul. Mira 19, 620002 Ekaterinburg, Russia; e-mail: r.n.maksimov@urfu.ru;
V.A. Shitov Institute of Electrophysics, Ural Branch, Russian Academy of Sciences, ul. Amundsena 106, 620016 Ekaterinburg, Russia;
M.R. Volkov, O.L. Vadimova, I.L. Snetkov Institute of Applied Physics, Russian Academy of Sciences, ul. Ul'yanova 46, 603950 Nizhny Novgorod, Russia

Received 27 April 2018
Kvantovaya Elektronika **48** (8) 695–698 (2018)
Translated by M.N. Basieva

For convenience, these compositions are hereinafter denoted as $Yb:Y_2O_3$ and $Yb:(Lu, Y)_2O_3$, respectively.

The synthesised $Yb:Y_2O_3$ and $Yb:(Lu, Y)_2O_3$ powders were calcined in air at a temperature of 900 °C–1100 °C for 3 h to transform the metastable structure of particles into the main cubic phase. The calcined particles were compacted into cylindrical samples 14 mm in diameter and 3–4 mm thick under a uniaxial pressure of 200 MPa. The compacts were sintered at a temperature of 1780 °C for 20 h at a residual gas pressure of $\sim 10^{-3}$ Pa. After sintering, the samples were bleached by annealing in air at a temperature of 1400 °C for 2 h and polished using diamond pastes with different grain sizes.

Figure 1 shows photographs of synthesised $Yb:Y_2O_3$ and $Yb:(Lu, Y)_2O_3$ ceramic samples ~0.2 mm thick and their transmission spectra measured on an SP-256 UFV spectrometer (LOMO). The dashed line in Fig. 1 corresponds to the theoretical Y_2O_3 transmission spectrum calculated using known refractive indices [18]. One can see that the measured transmission coefficients in the visible and near-IR spectral regions almost coincide with the calculated spectrum, which testifies to a high optical quality of the synthesised ceramics. A slight decrease in the transmission at wavelengths of 500–700 nm is caused by the presence of an insignificant amount of microstructural defects (pores) formed as a result of imperfect compaction of nanopowders.

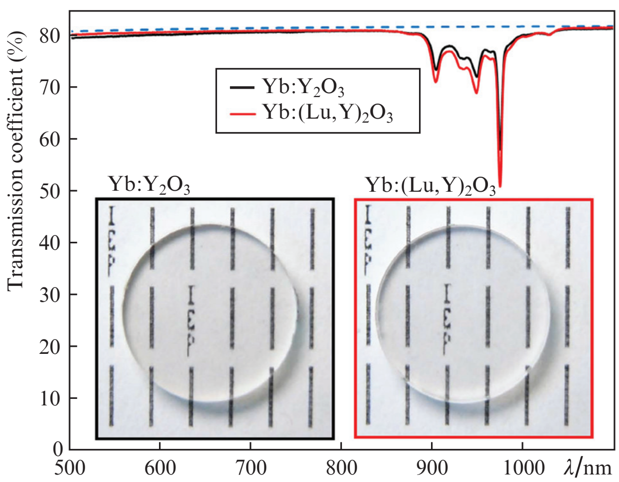

Figure 1. (Colour online) Transmission spectra of the synthesised ceramic samples and their photographs on a paper sheet with symbols demonstrating the absence of macrodefects in the samples. The dashed line corresponds to the theoretical spectrum of Y_2O_3.

When studying the spectral characteristics of the synthesised ceramics, we paid special attention to the analysis of the absorption and gain spectra, as well as to the measurement of the radiative lifetime of the upper laser level. The absorption cross sections were calculated using the expression

$$\sigma_{abs} = \frac{1}{NL}\ln\left[\frac{I_{in}(\nu)}{I_{out}(\nu)}\right], \quad (1)$$

where N is the concentration of dopant ions (cm^{-3}); L is the sample thickness; ν is the frequency, and $I_{in}(\nu)$ and $I_{out}(\nu)$ are the spectral intensities of the incident and passed radiation taking into account the Fresnel losses. The dopant concentration was determined by the formula

$$N = C_{Yb}\frac{2\rho}{Mm_p}, \quad (2)$$

where C_{Yb} is the known concentration of dopant ions in at %; ρ is the material density; M is the molar mass of the material, and m_p is the proton mass.

In turn, the gain spectra of synthesised ceramics were plotted using the McCumber method [19], which generalise the Einstein relation for absorption and stimulated emission cross sections σ_{em} to the case of strongly bound energy levels as

$$\sigma_{em}(\nu) = \sigma_{abs}(\nu)\frac{Z_{low}}{Z_{up}}\exp\left(\frac{E_{ZPL} - h\nu}{kT}\right), \quad (3)$$

where Z_{low} and Z_{up} are the partial functions of the ground and excited multiplets; E_{ZPL} is the energy difference between the lowest states of the ground and excited multiplets; h is the Planck constant; k is the Boltzmann constant; and T is the temperature. This method, despite its low accuracy in the long-wavelength region, makes it possible to estimate the shape of the gain spectrum.

The calculated absorption and gain spectra of synthesised $Yb:Y_2O_3$ and $Yb:(Lu, Y)_2O_3$ ceramics are shown in Fig. 2. Substitution of a part of Yb^{3+} cations by Lu^{3+} cations causes shifts of the absorption and luminescence peaks of Yb^{3+} ions in the yttrium oxide matrix. For example, the zero-phonon absorption peak shifts from wavelength $\lambda = 976.8$ nm to $\lambda = 976.4$ nm, while the gain band peaking at $\lambda = 1031.5$ nm shifts to longer wavelengths by 0.5 nm. In addition, with introduction of Lu_2O_3, the gain band at $\lambda = 1031$ nm broadens from 15 to 17 nm (at half maximum). Therefore, the calculated duration of generated laser pulses decreases from 104 to 92 fs.

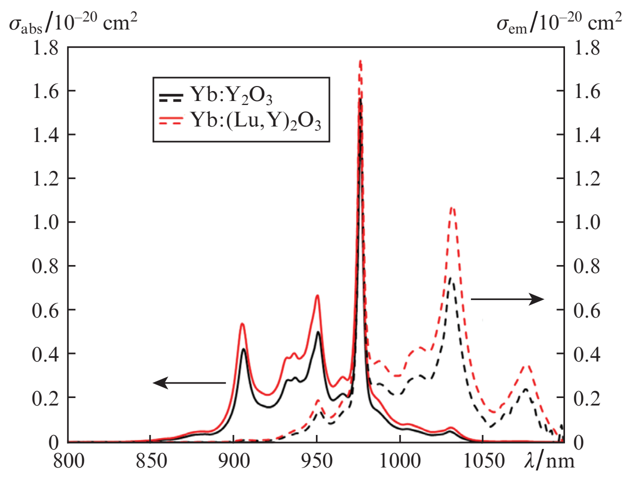

Figure 2. (Colour online) Calculated absorption (solid curves) and gain (dashed curves) spectra of synthesised ceramics.

The study of the luminescence decay kinetics at the $^2F_{5/2} \rightarrow {}^2F_{7/2}$ transition of Yb^{3+} ions showed that the radiative lifetimes of the $^2F_{5/2}$ level in the synthesised $Yb:Y_2O_3$ and $Yb:(Lu, Y)_2O_3$ ceramics almost coincide. The lifetimes were measured using a modified pinhole method [20, 21]. Pump radiation with $\lambda = 940$ nm was tightly focused on the studied sample, and the time for which the signal intensity decreased by e times was calculated depending on the diameter of the aperture restricting the viewing angle of the measuring diode.

Using linear approximation, the time corresponding to the completely closed aperture, i.e., to the radiative lifetime of the $^2F_{5/2}$ level, was determined to be 932 and 878 μs for $Yb:Y_2O_3$ and $Yb:(Lu, Y)_2O_3$ ceramics, respectively. These values agree with the value found previously for $Yb:Y_2O_3$ single-crystal films (860 μs) [22]. Thus, Lu_2O_3 and ZrO_2 additives have no negative effect on the radiative lifetime of the $^2F_{5/2}$ level of Yb^{3+} ions in yttrium oxide ceramics.

3. Laser oscillation

To perform experiments and design a disk laser, we used ceramic active elements ~200 μm thick. The faces of each sample were coated with dielectric films, i.e., one face was antireflection coated for the pump wavelength (940 nm) and the other face had a reflective coating for the lasing wavelength (1030 nm). The fabricated active elements were mounted on a diamond heat sink placed in a water-cooled laser head. The laser head was introduced into a laser cavity formed by the rear face of the active element and two dielectric mirrors, namely a spherical mirror (radius of curvature 120 cm) with a reflectivity of ~100% at λ = 1030 nm and a plane output mirror. As output mirrors, we used mirrors with reflectivities of 97%, 95%, and 90% at λ = 1030 nm. A Laserline LDM 2000 fibre-coupled diode laser emitting at λ = 940 nm was used as a pump source. The pump spot diameter was 5 mm. The scheme provided 12 V-shaped passes of pump radiation through the active element. The photograph of the laser cavity and the pump coupling system is presented in Fig. 3.

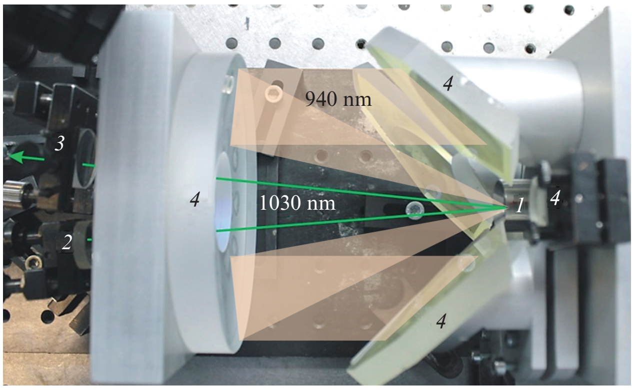

Figure 3. (Colour online) Photograph of the cavity and the pump coupling system: (*1*) active element; (*2*) spherical mirror; (*3*) output plane mirror; (*4*) system of mirrors for pump coupling.

Lasing for all output mirrors was achieved in a quasi-cw regime under pumping by 3.5-ms pulses with a repetition rate of 9.7 Hz. The dependences of the output laser power on the pump power are presented in Fig. 4. The maximum slope efficiency (32.3%) with an average power of 8 W was achieved in an $Yb:(Lu, Y)_2O_3$ sample with the use of an output mirror with a transmittance of 10%. The low lasing efficiency for the $Yb:Y_2O_3$ sample is related to destruction of the dielectric coating of the active element in the process of its mounting on the heat sink. Visual examination of the active element mounted on the heat sink revealed extended defects on the active element surface caused by partial peeling of the coating, which did not allow us to achieve better lasing characteristics with the used pump spot size.

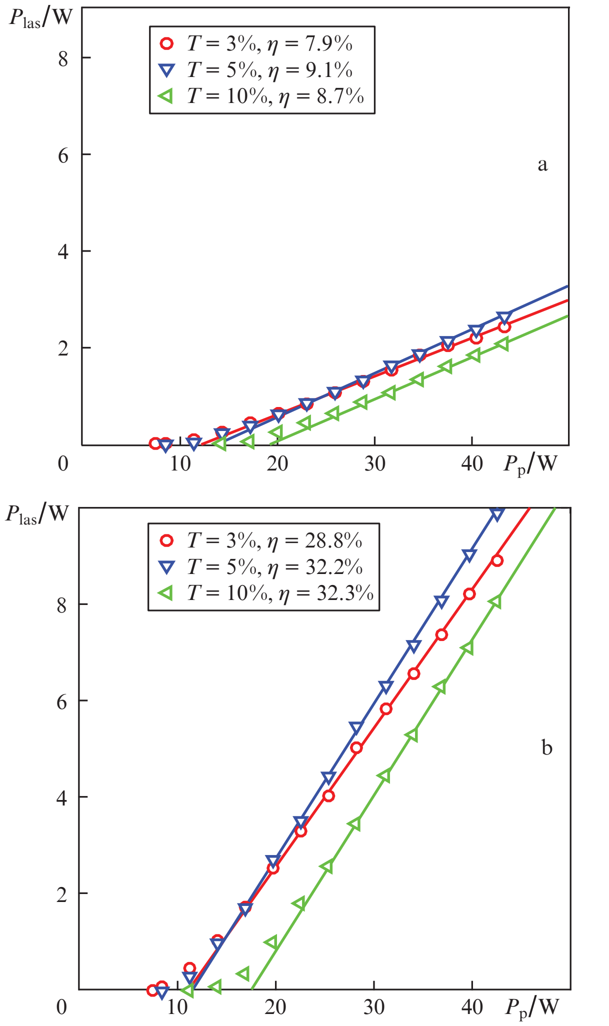

Figure 4. (Colour online) Dependences of the output laser power P_{las} on the pump power P_p for (a) $Yb:Y_2O_3$ and (b) $Yb:(Lu, Y)_2O_3$ ceramic thin disks at different output-mirror transmittances T and slope efficiencies η.

In addition, we measured the laser spectra at identical pump powers but different transmission coefficients of the output mirror (Fig. 5). Introduction of lutetium oxide into the $Yb:Y_2O_3$ matrix shifts the maximum of the laser spectrum to longer wavelengths and broadens its profile. In particular, in

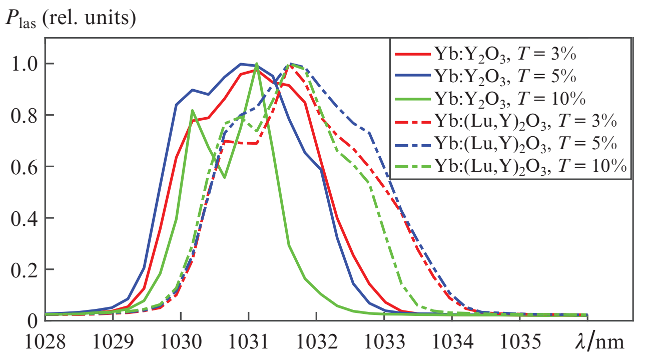

Figure 5. (Colour online) Normalised laser spectra of $Yb:Y_2O_3$ and $Yb:(Lu, Y)_2O_3$ ceramics at identical pump powers and different output mirror transmittances.

the case of an output mirror transmittance of 3%, the spectral width of laser radiation at half maximum increases from 2.4 to 2.6 nm for ceramics based on the solid solution of lutetium and yttrium oxides. The obtained active medium based on Yb:(Lu, $Y)_2O_3$ has a rather broad emission spectrum and a high optical quality and can be used for generation of ultrashort laser pulses.

4. Conclusions

We have studied the spectral, luminescent, and lasing properties of Yb:Y_2O_3 and Yb:(Lu, $Y)_2O_3$ solid solution ceramics fabricated by solid-phase vacuum sintering of nanopowders synthesised by laser ablation. The transmission coefficient of the samples 0.2 mm thick in the near-IR region reached 86.1%, which almost coincides with the theoretical value for Y_2O_3 (81.9%). It is shown that the substitution of a part of Y^{3+} cations by Lu^{3+} cations in amount of ~12% leads to a shift of the absorption and luminescence peaks of Yb^{3+} ion, as well as to broadening of the gain and lasing spectra. Repetitively pulsed laser radiation with a power of 8 W with a slope efficiency of 32.3% is demonstrated. The synthesised active medium based on the Yb:(Lu, $Y)_2O_3$ solid solution is promising for generation of ultrashort laser pulses.

Acknowledgements. This work was supported by the Russian Foundation for Basic Research (Project No. 17-308-50021 mol_nr).

References

1. Rath W., Brettschneider C. *Laser Tech. J.*, **11**, 23 (2014).
2. Richardson M. *Proc. Conf. on Lasers and Electro-Optics/Pacific Rim* (Busan, 2015) 25D3-1.
3. Malinauskas M., Žukauskas A., Hasegawa S., Hayasaki Y., Mizeikis V., Buividas R., Juodkazis S. *Light-Sci. Appl.*, **5**, 1 (2016).
4. National Ignition Facility & Photon Science. Lawrence Livermore National Laboratory; http://lasers.llnl.gov/.
5. HiPER. HiPER Project; http://hiper-laser.org/.
6. Laser Megajoule. The Megajoule Laser Facility; http://lmj.cea.fr/index-en.htm.
7. Garanin S.G., Dmitryuk A.V., Zhilin A.A., Mikhailov M.D., Rukavishnikov N.N. *Opt. Zh.*, **77**, 52 (2010).
8. Garanin S.G., Dmitryuk A.V., Zhilin A.A., Mikhailov M.D., Rukavishnikov N.N. *Opt. Zh.*, **78**, 60 (2011).
9. Sanghera J., Kim W., Villalobos G., Shaw B., Baker C., Frantz J., Sadowski B., Aggarwal I. *Materials*, **5**, 258 (2012).
10. Ikesue A., Aung Y.L. *Nat. Photonics*, **2**, 721 (2008).
11. Ikesue A., Aung Y.L., Taira T., Kamimura T., Yoshida K., Messing G.L. *Annu. Rev. Mater. Res.*, **36**, 397 (2006).
12. Tokurakawa M., Shirakawa A., Ueda K., Yagi H., Noriyuki M., Yanagitani T., Kaminskii A.A. *Opt. Express*, **17**, 3353 (2009).
13. Bagayev S.N., Osipov V.V., Shitov V.A., Pestryakov E.V., Kijko V.S., Maksimov R.N., Lukyashin K.E., Orlov A.N., Polyakov K.V., Petrov V.V. *J. Eur. Ceram. Soc.*, **32**, 4257 (2012).
14. Beil K., Saraceno C.J., Schriber C., Emaury F., Heckl O.H., Baer C.R.E., Golling M., Sudmeyer T., Keller U., Krankel C., Huber G. *Appl. Phys. B*, **113**, 13 (2013).
15. Jing W., Loiko P., Serres J.M., Wang Y., Vilejshikova E., Aguiló M., Díaz F., Griebner U., Huang H., Petrov V., Mateos X. *Opt. Mater. Express*, **7**, 4192 (2017).
16. Osipov V.V., Kotov Y.A., Ivanov M.G., Samatov O.M., Lisenkov V.V., Platonov V.V., Murzakaev A.M., Medvedev A.I., Azarkevich E.I. *Laser Phys.*, **16**, 116 (2006).
17. Osipov V.V., Platonov V.V., Lisenkov V.V., Podkin A.V., Zakharova E.E. *Phys. Status Solidi C*, **10**, 926 (2013).
18. Kaminskii A.A., Ueda K., Konstantinova A.F., Yagi H., Yanagitani T., Butashin A.V., Orekhova V.P., Lu J., Takaichi K., Uematsu T., Musha M., Shirokava A. *Crystallogr. Rep.*, **48**, 1041 (2003).
19. McCumber D.E. *Phys. Rev.*, **136**, A954 (1964).
20. Kühn H., Fredrich-Thornton S.T., Kränkel C., Peters R., Petermann K. *Opt. Lett.*, **32**, 1908 (2007).
21. Snetkov I.L., Zhou D., Yakovlev A.I., Volkov M.R., Kuznetsov I.I., Mukhin I.B., Palashov O.V., Shi Y., Ueda K. *Laser Phys. Lett.*, **15**, 035801 (2018).
22. Beecher S.J., Parsonage T.L., Mackenzie J.I., Sloyan K.A., Grant-Jacob J.A., Eason R.W. *Opt. Express*, **22**, 22056 (2018).